analytical chemistry

Article

Cite This: Anal. Chem. 2017, 89, 11122-11128

pubs.acs.org/ac

Improvement of LOD in Fluorescence Detection with Spectrally Nonuniform Background by Optimization of Emission Filtering

Victor A. Galievsky, Alexander S. Stasheuski, and Sergey N. Krylov*

Department of Chemistry and Centre for Research on Biomolecular Interactions, York University, Toronto, Ontario M3J 1P3, Canada

Supporting Information

ABSTRACT: The limit-of-detection (LOD) in analytical instruments with fluorescence detection can be improved by reducing noise of optical background. Efficiently reducing optical background noise in systems with spectrally nonuniform background requires complex optimization of an emission filter—the main element of spectral filtration. Here, we introduce a filter-optimization method, which utilizes an expression for the signal-to-noise ratio (SNR) as a function of (i) all noise components (dark, shot, and flicker), (ii) emission spectrum of the analyte, (iii) emission spectrum of the optical background, and (iv) transmittance spectrum of the emission filter. In essence, the noise components and the emission spectra are determined experimentally and substituted into the expression. This leaves a single variable—the transmittance spectrum of the filter—which is optimized numerically by maximizing SNR. Maximizing SNR provides an accurate way of filter optimization, while a previously used approach based on maximizing a signal-to-background ratio (SBR) is the approximation that can lead to much poorer LOD specifically in detection of fluorescently labeled biomolecules. The proposed filter-optimization method will be an indispensable tool for developing new and improving existing fluorescence-detection systems aiming at ultimately low LOD.

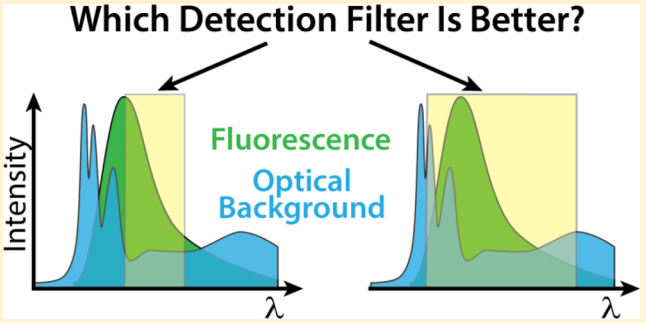

In analytical methods, fluorescence detection of an analyte can yield arguably the best limit-of-detection (LOD) without its preconcentration or enzymatic amplification and is a preferred approach when LOD is paramount.[1−4] LOD is affected by noise, especially optical noise occurring when optical background accompanies fluorescence of analyte. To evaluate the influence of both noise and analytical signal on LOD, signal-to-noise ratio (SNR) should be used as a figure of merit for fluorescence detection.[5−7] Accordingly, LOD can be improved via increasing analytical signal or decreasing optical background noise.

Increasing signal is mainly achieved by increasing power of the excitation light source (e.g., laser), which is expensive and may counter-productively raise optical background and, consequently, its noise. Useful signal also depends on optical collection efficiency, which is mainly defined by an optical scheme of choice.[5] Any improvement of collection efficiency is usually technically challenging and expensive; it also inevitably increases optical noise. Reducing optical noise requires efficient suppression of background light while preserving fluorescence of the analyte. There are numerous optical filtering techniques based on spectral, spatial, temporal, and polarization properties of light.[5,7−9] In the current work, we analyze the most effective method—spectral filtering—exploiting differences in spectra between analyte fluorescence and optical background to improve LOD.

The necessity to attenuate background light while keeping fluorescence unchanged constitutes an optimization problem: a transmittance spectrum of the optical filter should be adjusted to allow maximum SNR. This optimization procedure is a nontrivial task because background spectrum can be nonuniform owing to contributions of multiple components with different spectra (other fluorophores, scattering, autofluorescence). Moreover, the noise dependence on the background light intensity should be known for SNR calculation.

In fluorescence detection, noise originates from both optical and nonoptical sources. Any optical noise (either from analytical signal or optical background) contains shot and flicker components.[10,11] Shot noise is fundamental; it arises from photon nature of light and equals to the square root of the number of photons (signal intensity). Flicker noise is nonfundamental; it is usually caused by fluctuations in experimental variables (e.g., excitation photon flux or temperature). The flicker noise is proportional to signal intensity. Nonoptical noise components are independent of the optical signal and include dark noise of photodetector as well as noise in electronic circuits used for signal amplification/conversion.

Received: August 21, 2017
Accepted: September 13, 2017
Published: September 13, 2017

DOI: 10.1021/acs.analchem.7b03400
Anal. Chem. 2017, 89, 11122−11128

Previous efforts for improvement of spectral filtering have been made in two ways: (i) searching for the best emission filter[12] (or the best combination of excitation and emission filters)[13,14] from available "catalog" filters by trying them all and (ii) calculation of optimum filter parameters from analyte and background spectra using a computer algorithm.[15,16] In all these works, the nonlinear dependence of noise on background was disregarded and, signal-to-background ratio (SBR) was utilized instead of SNR as an optimization parameter. However, SBR is not a correct filter optimization parameter to get the best LOD; in analytical systems with strict LOD requirements the correct noise model must be taken into account.[17−20]

Here, we introduce a comprehensive approach for maximizing SNR in fluorescence detection with spectrally nonuniform background through the optimization of emission filter. This optimization would typically be performed when all steps are taken to minimize the background intensity, and further improvement of SNR can be done by fine-tuning of detection spectral window. The method includes measuring the emission spectra of analyte and optical background as well as finding the exact dependence of noise value on intensity of the optical signal. We have demonstrated the application of this method to optimize the filter in a commercial capillary-electrophoresis (CE) instrument with laser-induced-fluorescence (LIF) detection as a proof-of-concept. The applicability as well as limitations of the approximate approach based on maximizing SBR are discussed and compared with those of the proposed SNR maximization procedure. The quantitative SNR method can be applied to design efficient filters for any fluorophore detected in analytical setups especially aiming at ultimately low LOD.

EXPERIMENTAL SECTION

Reagents. Sodium fluorescein (MW 376.3, PN F6377) was obtained from Sigma-Aldrich and used without additional purification. Fluorescein concentration was determined spectrophotometrically using its molar absorption coefficient $\varepsilon_{490\ nm} = 76.9 \times 10^3\ M^{-1}cm^{-1}$.[21]

Capillary Electrophoresis. CE-LIF experiments were carried out using a P/ACE MDQ instrument (SCIEX, Concord, ON, Canada) equipped with a 488 nm solid-state continuous-wave laser Whisper IT W488-8PM (PIC, San Jose, CA, USA) and an excitation filter FF02-482/18 (Semrock, Rochester, NY, USA). Electrophoresis was done in a 30 cm long fused-silica capillary (Polymicro Technologies, Phoenix, AZ, USA) with an inner diameter of 75 μm and an outer diameter of 360 μm. The detector was placed 20 cm from the capillary inlet. Prior to every run, the capillary was rinsed sequentially with each of 100 mM HCl, 100 mM NaOH, deionized water, and electrophoresis run buffer (25 mM Borax at pH 9.2) at a pressure of 30 psi for 30 s. The samples were injected into the capillary by long pressure pulses of 0.5 psi ×40 s, which was required to generate wide peaks with a flat plateau on the top. Electrophoresis was carried out with an electrical potential of +25 kV applied to the injection end of the capillary; the output of the capillary was grounded. The temperature of the capillary coolant was set to 15 °C.

Fluorescence signal E and baseline $E_B + E_D$ (consisting of the optical background E_B and the dark signal E_D) were determined by averaging at least 60 data points on the peak top and the baseline, respectively (Figure 1). Total and baseline noise values were calculated as standard deviation (SD) of the corresponding data points. Precision of noise parameters was determined as SD of the values obtained from 9 experimental data sets. All CE-LIF signals were recorded in relative fluorescence units (RFU). One RFU approximately corresponds to a signal of 1 nM fluorescein in our electrophoresis run buffer measured in a capillary with 75 μm inner diameter. The "dynamic range" parameter in 32 Karat, version 7.0 software (SCIEX, Concord, ON, Canada), was set to 1 RFU and a data acquisition frequency was 4 Hz. In the following, we refer to an optical filter set (notch 488 nm and bandpass 520 nm filters) installed by the manufacturer in the CE-LIF module of P/ACE MDQ (SCIEX, Concord, ON, Canada) as the "original filter". "530/40 nm" refers to a combination of four filters, that is, two FF01-535/50 and two FF03-525/50 filters (Semrock, Rochester, NY, USA). Transmission spectra of all filters were measured using LAMBDA 950 UV/vis/NIR spectrophotometer (PerkinElmer, Woodbridge, ON, Canada).

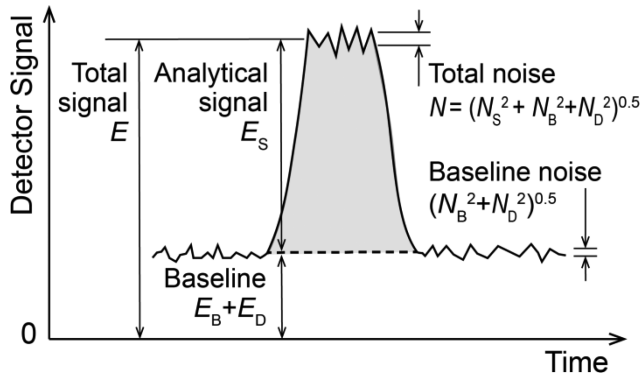

Figure 1. Schematic depiction of signals and noises in fluorescence measurements. The analytical signal E_S is a change in the detector response due to the presence of analyte. The baseline is the detector response during a measurement without analyte; the baseline consists of the optical background E_B and the dark signal E_D. Noises N, N_S, N_B, and N_D are SD of E, E_S, E_B, and E_D, respectively.

Spectroscopy. Spectra (in photon·nm^{-1}) were obtained using a CCD camera DV401-BV SH (Andor, Concord, MA, USA) cooled down to −20 °C. The camera was coupled with Shamrock 163 spectrograph (Snowhouse Solution, Lac-Beauport, QC, Canada) equipped with 600 lines/mm grating (blaze wavelength at 500 nm). Dark signal was subtracted from the raw spectra. The system was spectrally calibrated using Hg and Ne lamps, and corrected to detector spectral responsivity by the standard light source SL1-CAL (StellarNet, Tampa, FL, USA). For spectral measurements, a photomultiplier tube (PMT) in the LIF detector was replaced with an optical fiber coupled with the F220SMA-A collimator (Thorlabs, Newton, NJ, USA) at the fiber's end. A 488 nm notch filter (SCIEX, Concord, ON, Canada) was set in front of the collimator, to avoid detector overloading by Rayleigh scattering. The spectra were converted to RFU·nm^{-1} units under an assumption that the integral of product of optical background spectrum with transmittance spectrum of the original filter is equal to the CE-LIF baseline value of 0.068 RFU. Measurements were sequentially done for the electrophoresis run buffer and a 10 nM solution of fluorescein that were propagated through the capillary by a constant pressure of 10 psi.

RESULTS AND DISCUSSION

Theoretical Background: SNR in Fluorescence Detection. The detection performance of an analytical instrument can be characterized by two main figures of merit: LOD and

DOI: 10.1021/acs.analchem.7b03400
Anal. Chem. 2017, 89, 11122−11128

precision. LOD is the smallest quantity of an analyte that can be detected with a defined probability of false positive and false negative errors.[22] Precision describes the distribution of the results of measurements around their mean value.[23,24] Both figures of merit are interconnected because in mathematical terms their definitions include values of noise and mean signal. Therefore, LOD and precision can be improved simultaneously through maximizing SNR.

SNR in fluorescence detection is defined as a ratio between the analytical signal E_S and the total noise N:

$$\mathrm{SNR} = \frac{E_S}{N} = \frac{E - (E_B + E_D)}{N} \tag{1}$$

where E_S is the difference between the total signal E and the baseline $E_B + E_D$ consisting of the optical background E_B and the dark signal E_D; N is a function of E_S, E_B, and E_D (Figure 1).

Thus, to evaluate SNR we need to find E_S, E_B, E_D, and function $N(E_S, E_B, E_D)$. E_S is obtained by integrating the product of fluorescence spectrum $[\tilde{E}(\lambda) - \tilde{E}_B(\lambda)]$ with the quantum efficiency $Q(\lambda)$ of the photodetector and the filter transmittance $T(\lambda)$

$$E_S = \int_\lambda [\tilde{E}(\lambda) - \tilde{E}_B(\lambda)]Q(\lambda)T(\lambda)\,\mathrm{d}\lambda \tag{2}$$

where $\tilde{E}(\lambda)$ and $\tilde{E}_B(\lambda)$ are emission spectra of the analyte and the optical background, respectively. A similar expression can be obtained for the optical background E_B

$$E_B = \int_\lambda \tilde{E}_B(\lambda)Q(\lambda)T(\lambda)\,\mathrm{d}\lambda \tag{3}$$

Using eqs 1−3 and taking into account the fact that E_D does not depend on λ, the following expression can be written for SNR:

$$SNR = \frac{\int_\lambda [\tilde{E}(\lambda) - \tilde{E}_B(\lambda)]Q(\lambda)T(\lambda)\,\mathrm{d}\lambda}{N(\tilde{E}(\lambda), \tilde{E}_B(\lambda), Q(\lambda), T(\lambda), E_D)} \tag{4}$$

The most favorable filter transmittance $T(\lambda)$ can be found by a numerical optimization algorithm, in which $T(\lambda)$ is varied to maximize *SNR*. Functions $\tilde{E}(\lambda)$, $\tilde{E}_B(\lambda)$, $Q(\lambda)$, and $N(\tilde{E}(\lambda), \tilde{E}_B(\lambda), Q(\lambda), T(\lambda), E_D)$ have to be determined for eq 4 to be used in calculations. In general, finding an exact mathematical form of eq 4 is a complex task, because an explicit form of $N(\tilde{E}(\lambda), \tilde{E}_B(\lambda), Q(\lambda), T(\lambda), E_D)$ is not known a priori. However, this can be done for a particular fluorescence setup by using some assumptions and special measurements.

Instrumental Model. CE-LIF instrument was chosen as a model fluorescence setup to examine the proposed filter-optimization method. CE-LIF can work with small-volume samples and analyze low-concentration analytes. Accordingly, CE-LIF is used for such challenging analytical tasks as detection of low-concentration bioanalytes in affinity assays and kinetic studies of target-ligand binding characterized by very low values of the equilibrium dissociation constant.[25−28] As a result, as low as possible LOD values are often demanded for CE setups.[29] LOD improvement in CE-LIF is, however, limited by significant noise of optical background, which is spectrally nonuniform and usually overlaps with fluorescence spectrum of the analyte.[5,30]

Most analytical instruments with fluorescence detection, including our tested commercial CE-LIF instrument, are equipped with analog photodetectors. The theory of noise in such detectors was developed in details to optimize experimental conditions in fluorescence spectrometry.[23,31] As a first approximation, all noises in an analog detector are considered independent and, consequently, a denominator in eq 4 may be presented as[5,23]

$$N = \sqrt{N_D^2 + N_B^2 + N_S^2} = \sqrt{[\kappa E_D + \sigma_{dex}^2 + \sigma_{ar}^2] + [\kappa E_B + (\chi_B E_B)^2] + [\kappa E_S + (\chi_S E_S)^2]} \tag{5}$$

Here, N_D, N_B, and N_S are nonoptical, background, and analytical-signal noises, respectively; κ is the shot noise coefficient; χ_S and χ_B are flicker factors (relative SD of fluctuations in photon flux due to flicker noise) of analytical signal and background, respectively; σ_{dex} is the SD of the dark-current excess noise, σ_{ar} is the SD of the amplifier-readout noise. All parameters in the 3 square-bracketed terms must be found for eq 5 to be substituted into the denominator in eq 4. Note that photon-counting mode is also used in analytical instruments with fluorescence detection, and for photon-counting detectors, noise expression can be written in a form similar to eq 5.[23]

Dark Noise. The first term $[\kappa E_D + \sigma_{dex}^2 + \sigma_{ar}^2]$ in the eq 5 contains components, which are always present and do not depend on the intensity of excitation light or the presence of a sample. If experimental conditions (temperature, PMT voltage, etc.) are constant, then $N_D = (\kappa E_D + \sigma_{dex}^2 + \sigma_{ar}^2)^{0.5}$ is a constant. N_D can be measured for a given instrument as the detector's noise, without any excitation light ($E_B = E_S = 0$). For our CE-LIF instrument N_D was found to be $(6.1 \pm 0.3) \times 10^{-6}$ RFU.

Optical Background Noise. The components in the second term $[\kappa E_B + (\chi_B E_B)^2]$ in eq 5 characterize optical background: κE_B describes shot noise and $(\chi_B E_B)^2$ defines flicker noise. The relative contribution of shot and flicker components to the background noise is a unique feature for every fluorescence setup, and has to be found experimentally. For this purpose, the dependence of N on E_B was measured (Figure 2) without any analyte ($E_S = 0$). E_B was in turn obtained from the measured baseline $E_B + E_D$ by subtracting from it the dark signal $E_D = 2.4 \times 10^{-4}$ RFU. The flicker factor χ_B and the shot-noise coefficient κ are target parameters, which can be found by fitting the experimental data in Figure 2 with the following function:

$$N = \sqrt{N_D^2 + \kappa E_B + (\chi_B E_B)^2} \tag{6}$$

Here, N_D is dark noise (determined previously) and E_B is a variable, which linearly depends on excitation power (Figure S1).

The shot-noise coefficient $\kappa = (1.4 \pm 0.4) \times 10^{-7}$ RFU was obtained. It is an instrument-defined constant, which also can be estimated independently from the known PMT and electronic amplifier parameters (see Table S1). In this way, we calculated $\kappa = 1.5 \times 10^{-7}$ RFU, which is in good agreement with the experimentally measured value.

Optical background noise prevails over dark noise. For example, N_B is almost 20 times greater than N_D at a standard laser excitation power of ~3.1 mW (Figures 2, as well as Figure S2 and Table S2). This result confirms an accepted assumption that light is the main source of noise in modern CE-LIF detectors.[6]

Analytical Signal Noise. The third term $[\kappa E_S + (\chi_S E_S)^2]$ in eq 5 describes noise N_S related to the analytical signal E_S

DOI: 10.1021/acs.analchem.7b03400
Anal. Chem. 2017, 89, 11122−11128

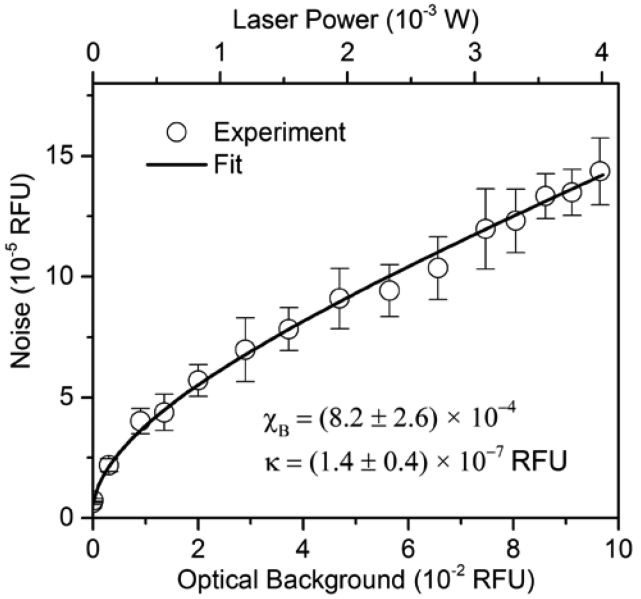

Figure 2. Noise dependence on the value of optical background E_B (circles). The solid line represents fitting the experimental data with eq 6 using χ_B and κ as target parameters. Optical background was varied via changing the laser power.

(Figure 1). Similar to the optical background noise, the noise from analytical signal consists of two components κE_S and $(\chi_S E_S)^2$ corresponding to shot and flicker noises, respectively. Here, only the flicker factor χ_S is an unknown and has to be obtained experimentally. The dependence of N on the analytical signal E_S was determined (Figure 3), and the following function was used for its fitting:

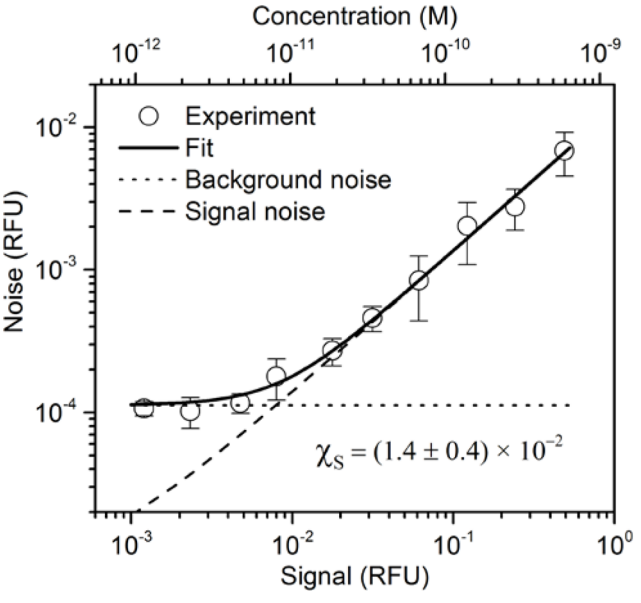

Figure 3. Noise dependence on the analytical signal E_S. E_S was varied by changing fluorescein concentration. Laser power was 3.1 mW that corresponds to $E_B = (6.8 \pm 0.6) \times 10^{-2}$ RFU. The solid line represents fitting the experimental data with eq 7 using χ_S as a target parameter. The dotted line is the background noise fraction calculated using eq 7 and $E_S = 0$. The dashed line is the analytical-signal-noise fraction calculated using eq 7 and $E_B = 0$. Signal is a linear function of the fluorescein concentration (see Figure S3).

$$N = \sqrt{N_D^2 + (\chi_B E_B)^2 + \kappa(E_B + E_S) + (\chi_S E_S)^2} \quad (7)$$

E_S was a variable changed experimentally by injecting fluorescein solutions in a range of concentrations from 1 to 620 pM under a constant intensity of excitation light, that is, when E_B = const.

At low signal magnitudes the noise does not change significantly because it is mainly defined by background noise. Note that optical background as well as its noise is constant in the current experiment as the light source power does not change. However, the solid curve in Figure 3 is greatly altered at signal values of approximately 10^{-2} RFU (corresponding to a fluorescein concentration of 10 pM). Analytical-signal noise (or rather, its flicker component) dominates for concentrations higher than 10 pM, and the total noise becomes proportional to the signal value. This means that the precision of measurements does not improve with growing analyte concentration.

Measurement of Emission Spectra. For spectral measurements, light was collected in the same spot inside the LIF module where the PMT photocathode is located. Thus, all possible sources of optical background including instrument's optics could be taken into account. Figure 4 shows the obtained fluorescence spectra of fluorescein $\tilde{E}_S(\lambda)$ and the nonuniform optical background $\tilde{E}_B(\lambda)$.

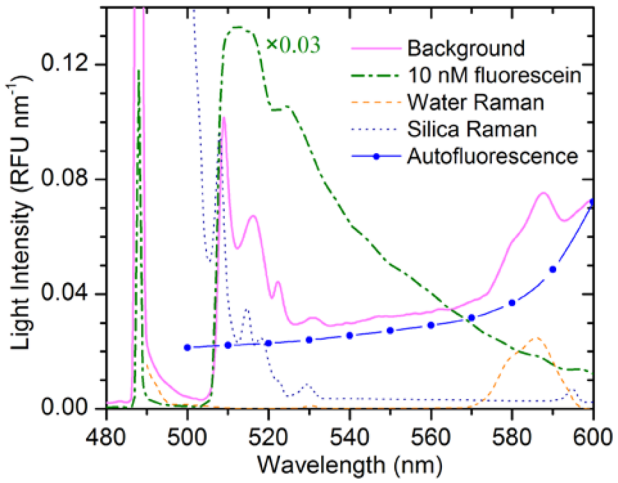

Figure 4. Emission spectra of fluorescein and background including its components. Spectrum $\tilde{E}_S(\lambda)$ of 10 nM fluorescein is obtained by subtraction of the background spectrum $\tilde{E}_B(\lambda)$ from the measured spectrum $\tilde{E}(\lambda)$. Spectra $\tilde{E}(\lambda)$ and $\tilde{E}_B(\lambda)$ were recorded through the 488 nm notch filter at a laser excitation power of 3.1 mW. Raman scattering spectra of water and silica were taken from the literature data and scaled to fit background peaks. The spectrum of autofluorescence was estimated as a difference between background and Raman spectra.

The spectrum of fluorescein solution above 505 nm is similar to the published results in the literature.[21] The sharp drop of measured signals to the left of 505 nm is caused by the transmittance profile of the excitation-blocking notch filter. The spectrum of the optical background is nonuniform, and for convenience it may be divided into four components: (i) a narrow and intense line near 488 nm; (ii) a short-wavelength intense band between 505 and 530 nm with several narrow lines; (iii) a distinct band at 570–600 nm; and (iv) a wide nonstructured band with slowly rising intensity toward long wavelengths.

DOI: 10.1021/acs.analchem.7b03400
Anal. Chem. 2017, 89, 11122–11128

Component (i) is caused by elastic Rayleigh scattering and reflection of laser light. The intensity of the scattered light is several orders of magnitude greater than the fluorescence intensity of the analyte, so the Rayleigh scattering must be heavily reduced by setting the notch and fluorescence bandpass filters. The spectrum of Rayleigh scattering is the same as that of excitation source. Common lasers used in CE-LIF have narrow emission lines, which lie far from the fluorescence spectra of analytes under study, thus spectral filtering of detected light allows almost complete elimination of Rayleigh scattering. If the excitation source has a wide emission spectrum, which spreads out of the blocking range of notch-filter, Rayleigh scattering can interfere with the analyte fluorescence. In such a case, an additional filter narrowing the excitation spectrum has to be used for SNR improvement (see Figure S4 and ref 9).

Band (ii) consists mainly of inelastic Raman lines of fused silica, which is a material of capillary walls. Band (iii) corresponds to water Raman band. We used nonpolarized Raman spectra taken from the literature.[32,33] Relative intensities of Raman spectra were adjusted to fit the background peaks (Figure 4). A spectrum of Raman scattering usually has the most intense lines close to the excitation laser line. Nevertheless, many Raman lines may fall into the spectral interval of analyte's fluorescence. This type of optical background may potentially be greatly reduced by using a filter with the optimal bandpass position.

The wide band (iv) is autofluorescence from an unidentified sources. Such wide and nonstructured band was not observed in another homemade CE-LIF setup (Figure S5). We suppose that band (iv) belongs to luminescence of sapphire ball-lens used in the collection optics of the commercial instrument tested. The ball lens is tightly attached to the capillary surface[34] and likely illuminated by the excitation laser beam. Autofluorescence is probably caused by sapphire impurities.[35]

A correct interpretation of the obtained nonuniform background spectra may significantly help in improving LIF detection. For example, if Raman lines overlap with the fluorescence spectrum of the analyte, then using another excitation wavelength may shift these lines outside the analyte spectrum.

Calculation of Optimal Bandpass Filter. Modern bandpass optical filters have nearly rectangular transmittance shape,[36] so it is safe to assume that a target filter can be described by a transmittance function $T(\lambda)$ with spectral boundaries at λ_1 and λ_2:

$$T(\lambda) = \begin{cases} 0 & \text{if} \quad \lambda < \lambda_1 \\ 1 & \text{if} \quad \lambda_1 \le \lambda \le \lambda_2 \\ 0 & \text{if} \quad \lambda > \lambda_2 \end{cases} \tag{8}$$

Using eqs 2, 3, and 8, we obtained the following equations for analytical signal and background ${E_S}^{\lambda_{1,2}}$ and ${E_B}^{\lambda_{1,2}}$, respectively, calculated in a spectral interval from λ_1 to λ_2

$${E_S}^{\lambda_{1,2}} = \int_{\lambda_1}^{\lambda_2} [\tilde{E}(\lambda) - \tilde{E}_B(\lambda)] Q(\lambda)\, d\lambda \tag{9}$$

$${E_B}^{\lambda_{1,2}} = \int_{\lambda_1}^{\lambda_2} \tilde{E}_B(\lambda) Q(\lambda)\, d\lambda \tag{10}$$

$Q(\lambda)$—quantum efficiency of the detector—was obtained by digitizing the corresponding plot in the specification of PMT used (Hamamtsu R5984). We assume that noise parameters (κ, χ_B, and χ_S) do not change significantly within fluorescein emission spectrum. Using eqs 4, 5, 9, and 10, SNR can be expressed through the known noise parameters and emission spectra of the analyte and the optical background:

$$\mathrm{SNR}^{\lambda_{1,2}} = \frac{{E_S}^{\lambda_{1,2}}}{\sqrt{{N_D}^2 + (\chi_B {E_B}^{\lambda_{1,2}})^2 + \kappa({E_B}^{\lambda_{1,2}} + {E_S}^{\lambda_{1,2}}) + (\chi_S {E_S}^{\lambda_{1,2}})^2}} \tag{11}$$

The evolutionary algorithm (Solver add-in, Microsoft Excel) was used for maximization of SNR expressed by eq 11 (utilizing ${E_S}^{\lambda_{1,2}}$ and ${E_B}^{\lambda_{1,2}}$ from eqs 9 and 10) via varying parameters λ_1 and λ_2. The search for optimum λ_1 and λ_2 was carried out within a range of 500−600 nm. As a result, an optimal filter for 1 pM fluorescein has a bandpass center at 528 nm and a width of 35 nm (528/35 nm, which is shown in Figure 5 as SNR-calculated filter).

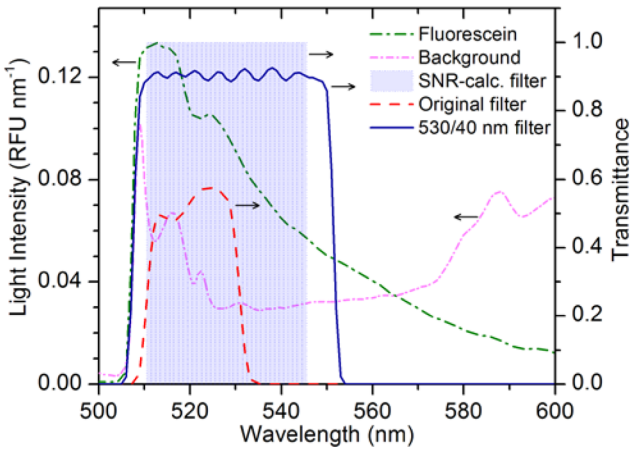

Figure 5. Emission spectra of fluorescein and optical background, as well as transmittance spectra of the optimal filter calculated using SNR maximization method, original bandpass filter mounted in the CE-LIF instrument, and the bandpass filter 530/40 nm having the bandwidth similar to the optimum value obtained by SNR maximization.

Equation 11 describes the total noise including the noise of analytical signal; therefore, the effect of analyte amount on the optimal filter parameters can be investigated. The calculated parameters are independent of the analyte concentration in a range of 1−10 pM (Figure S6A). At higher concentrations, the filter bandwidth increases and the center position shifts to the longer wavelengths. The comparison of optimal filters for 1 pM fluorescein (528/35 nm) and 4 nM fluorescein (550/100 nm) shows their similarity in terms of SNR (or precision, which is a reciprocal of SNR) for concentrations higher than 10 pM (Figure S6B). Consequently, the calculated filter 528/35 nm provides better precision for the picomolar concentration range (e.g., 1.4 times for 1 pM) and keeps high precision for sub-nanomolar and nanomolar concentrations.

The transmittance spectrum of the SNR-calculated filter (528/35 nm), as well as the spectra of the original filter (520/20 nm) installed by the CE-instrument manufacturer and a new filter (530/40 nm), are shown in Figure 5. The filter 530/40 nm was assembled from several bandpass filters to get a transmittance spectrum as similar as possible to the calculated one.

DOI: 10.1021/acs.analchem.7b03400
Anal. Chem. 2017, 89, 11122−11128

LOD Measurement. In analytical separation methods (e.g., chromatography and electrophoresis), an analyte peak as well as a pure baseline are detected in the same run. As a result, LOD estimation can be carried out through signal-to-baseline-noise ratio (SN_BR) calculated as a ratio between the analytical signal (usually the peak height) and the baseline noise (SD of the baseline). The LOD is determined as an analyte concentration resulting in an SN_BR value of 3.[37] For concentrations near LOD, the SNR value is equal to the SN_BR value (Table S2 and Figure S7).

Fluorescein LOD was calculated from the SN_BR dependence on analyte concentration in ranges of 1−620 and 1−310 pM, for the original and 530/40 nm filters, respectively (Figures S3 and S8). Typical electropherograms of 1 pM fluorescein obtained using the 530/40 nm filter are shown in Figure S9. An LOD value of 0.42 ± 0.05 pM was estimated with the original filter (520/20 nm). Two times better LOD value of 0.20 ± 0.01 pM was obtained with the filter 530/40 nm. Note, LOD improvement is based on both better transmission and optimized spectral window (bandwidth and center position) of the filter 530/40 nm in comparison to the original filter (520/20 nm). For a virtual 520/20 nm filter with transmission increased from 50% to 90% (similar to that of the optimal 530/40 nm filter), the signal and the optical background rise by a factor of 1.8 (90/50). In this case, the optical background noise rises by a factor of 1.6 as can be calculated from Figure S2. As a result, SN_BR (LOD) improvement is only 1.1 (1.8/1.6) times for the virtual 520/20 nm filter with the increased transmission. Therefore, a total LOD enhancement of 2.1 times (0.42 pM/0.20 pM) obtained with the optimal 530/40 nm filter was mainly due to the optimized spectral window. Thus, the benefits from the optimized window and the increased transmission were 1.9 and 1.1 times, respectively.

The reported filter optimization is the easiest way of further improving LOD as there is no other simple way to reduce the optical background in the studied commercial CE instrument except for spectral filtration. The CE-LIF module, equipped with a fast ball lens and a concave reflector, was designed by the instrument manufacturer specifically for the greatest fluorescence-collection efficiency (up to 40%).[34] Such an optical scheme does not allow the use of effective spatial filtration for the minimization of scattered light from the walls of the capillary.

If the background noise is dominated by the shot noise, an additional way to improve LOD without a considerable modification of an LIF setup is increasing the laser power, until photobleaching is reached.[5,38,39] Let us estimate SN_BR growth and corresponding LOD improvement that can be achieved in our CE-LIF setup with an excitation power rise. At a laser power of 3.1 mW, which is typical for a P/ACE MDQ instrument, the shot-noise component is about two times higher than the flicker noise component as seen in Figure S2. The dependence of total noise N on the excitation power is slightly faster than a square root function, in contrast to the analytical signal E_S, which is linearly proportional to the laser light intensity. As a result, the growth of excitation power can improve SN_BR and consequently LOD. However, this enhancement is not effective because the contribution of the flicker component rises rapidly and inhibits the SN_BR gain at larger powers. For example, a 4-fold increase in the excitation power, which can be achieved by purchasing a new expensive laser, would only lead to SN_BR increase of 1.5 times (Figure S2). Note, the flicker component in background noise mainly originates from the fluctuation of laser intensity. Therefore, if optical noise is dominated by flicker noise, LOD improvement can be reached by using high-stability lasers or laser amplitude stabilizers (noise-eaters).

SNR and SBR Comparison. A simplified approach based on SBR maximization can only produce acceptable results if (i) the flicker component is predominant in the optical noise or (ii) background has a uniform (flat) spectrum within the analyte's fluorescent band. Using SBR maximization can lead to a large decrease in the efficiency of the optical filter in comparison to the SNR optimization, if optical background is spectrally nonuniform and optical noise is dominated by the shot component (which is usually true for low-intensity laser excitation).[6] Our estimation shows that the difference in the calculated values of SNR (and LOD, respectively) for the filters can reach an order of magnitude, when the optical noise is shot-dominated and the spectrum of the optical background has a shape similar to useful fluorescence spectrum with a slightly shifted maximum (see Figure S10). Such spectrally nonuniform background can be observed when detecting fluorescently labeled biomolecules in the presence of the unreacted fluorophore. In such a case fluorescence from the target-conjugated fluorophore (useful signal) interferes with the emission of the unbound and/or nonspecifically bound fluorophore (optical background).[40,41] Still, the SBR-maximization approach can result in a satisfactory spectral filtering; therefore, a decision about suitability of SBR as a filter optimization parameter should be taken individually for every case. Note, the SNR-maximization approach provides accurate results for all experimental conditions, and it is especially recommended when the lowest LOD is required.

Concluding Remarks. A quantitative method is proposed for LOD improvement in fluorescence detection by finding the optimal emission bandpass filter. The method is based on calculation of the filter bandpass using SNR as the optimization parameter, where the SNR expression is built using measured noise parameters and spectra of the analyte and optical background. Unlike simplified methods, such as SBR-based optimizations, which can lead to a filter with an unacceptably low SNR (and, consequently, unacceptably high LOD), the proposed method is accurate and allows one to get maximum effectiveness of spectral filtering in fluorescent detection. The method can be applied for LOD improvements in existing setups, as well as for finding the best filters for new fluorescence instruments.

■ ASSOCIATED CONTENT

Supporting Information

The Supporting Information is available free of charge on the ACS Publications website at DOI: 10.1021/acs.analchem.7b03400.

Dependences of background on laser power; dependences of noise on optical background; dependences of signal, noise, SNR, SN_BR, filter center, and filter fwhm on fluorescein concentration; analysis of experimental and simulated spectra of fluorescence signal and optical background; typical electropherograms, noise parameters, and SNR components obtained for the CE-LIF instrument (PDF)

DOI: 10.1021/acs.analchem.7b03400
Anal. Chem. 2017, 89, 11122−11128

AUTHOR INFORMATION

Corresponding Author

*E-mail: skrylov@yorku.ca.

ORCID

Sergey N. Krylov: 0000-0003-3270-2130

Author Contributions

The manuscript was written through contributions of all authors. All authors have given approval to the final version of the manuscript.

Notes

The authors declare no competing financial interest.

ACKNOWLEDGMENTS

The authors thank the Natural Sciences and Engineering Research Council of Canada for support: Discovery grant to S.N.K. The authors thank Dr. Sven Kochmann and Dr. Mirzo Kanoatov for reading the manuscript and providing critical comment.

REFERENCES

(1) Harvey, D. In *Modern Analytical Chemistry*; McGraw-Hill Higher Education: Boston, 2000; pp 368−460.
(2) Lingeman, H.; Underberg, W. J. M.; Takadate, A.; Hulshoff, A. *J. Liq. Chromatogr.* **1985**, *8*, 789−874.
(3) Scanlan, C.; Lapainis, T.; Sweedler, J. V. In *Handbook of Capillary and Microchip Electrophoresis and Associated Microtechniques*; Landers, J. P., Ed.; CRC Press, Taylor & Francis Group: Boca Raton, 2008; pp 305−334.
(4) Dovichi, N. J. *TrAC, Trends Anal. Chem.* **1984**, *3*, 55−57.
(5) Galievsky, V. A.; Stasheuski, A. S.; Krylov, S. N. *Anal. Chim. Acta* **2016**, *935*, 58−81.
(6) Johnson, M. E.; Landers, J. P. *Electrophoresis* **2004**, *25*, 3513−3527.
(7) Dovichi, N. J.; Martin, J. C.; Jett, J. H.; Trkula, M.; Keller, R. A. *Anal. Chem.* **1984**, *56*, 348−354.
(8) Seitzinger, N. K.; Hughes, K. D.; Lytle, F. E. *Anal. Chem.* **1989**, *61*, 2611−2615.
(9) Dodgson, B. J.; Krylov, S. N. *TrAC, Trends Anal. Chem.* **2012**, *33*, 23−34.
(10) Alkemade, C. T. J.; Snelleman, W.; Boutilier, G. D.; Pollard, B. D.; Winefordner, J. D.; Chester, T. L.; Omenetto, N. *Spectrochim. Acta, Part B* **1978**, *33*, 383−399.
(11) Boutilier, G. D.; Pollard, B. D.; Winefordner, J. D.; Chester, T. L.; Omenetto, N. *Spectrochim. Acta, Part B* **1978**, *33*, 401−416.
(12) Moretto, C.; Kiefer, J. In *Lasers, Sources, and Related Photonic Devices*; OSA Technical Digest: San Diego, USA, 2012; p LT6B.2.
(13) de Jong, E. P.; Lucy, C. A. *Anal. Chim. Acta* **2005**, *546*, 37−45.
(14) Roy, M.; Dadani, F.; Niu, C. J.; Kim, A.; Wilson, B. C. *J. Biomed. Opt.* **2012**, *17*, 026002.
(15) Galbraith, W.; Ernst, L. A.; Taylor, D. L.; Waggoner, A. S. *Proc. SPIE* **1989**, *1063*, 74−122.
(16) Anderson, N.; Prabhat, P.; Erdogan, T. *White Paper: Spectral Modeling in Fluorescence Microscopy*; Semrock, Inc.: Rochester, NY, 2015. http://www.semrock.com/Data/Sites/1/semrockpdfs/spectral_modeling_in_fluorescence_microscopy.pdf (accessed August 1, 2017).
(17) McCarthy, W. J.; Winefordner, J. D.; St. John, P. A. *J. Chem. Educ.* **1967**, *44*, 80.
(18) Bower, N. W.; Ingle, J. D. *Appl. Spectrosc.* **1981**, *35*, 317−324.
(19) Aramburu, I.; Galban, J.; Ostra, M.; Ubide, C.; Vidal, M.; Zuriarrain, J. *Anal. Methods* **2015**, *7*, 2379−2385.
(20) Sadler, D. A.; Littlejohn, D.; Perkins, C. V. *J. Anal. At. Spectrom.* **1996**, *11*, 207−212.
(21) Sjoback, R.; Nygren, J.; Kubista, M. *Spectrochim. Acta, Part A* **1995**, *51*, L7−L21.
(22) Currie, L. A. *Pure Appl. Chem.* **1995**, DOI: 10.1351/pac199567101699.
(23) Ingle, J. D.; Crouch, S. R. In *Spectrochemical Analysis*; Prentice-Hall, Inc.: NJ, 1988; pp 1−12, 135−163.
(24) Danzer, K. In *Analytical Chemistry. Theoretical and Metrological Fundamentals*; Springer: Berlin, 2007; pp 176−216.
(25) Dodgson, B. J.; Mazouchi, A.; Wegman, D. W.; Gradinaru, C. C.; Krylov, S. N. *Anal. Chem.* **2012**, *84*, 5470−5474.
(26) Wegman, D. W.; Ghasemi, F.; Stasheuski, A. S.; Khorshidi, A.; Yang, B. B.; Liu, S. K.; Yousef, G. M.; Krylov, S. N. *Anal. Chem.* **2016**, *88*, 2472−2477.
(27) Kanoatov, M.; Galievsky, V. A.; Krylova, S. M.; Cherney, L. T.; Jankowski, H. K.; Krylov, S. N. *Anal. Chem.* **2015**, *87*, 3099−3106.
(28) Kanoatov, M.; Mehrabanfar, S.; Krylov, S. N. *Anal. Chem.* **2016**, *88*, 9300−9308.
(29) Wu, S.; Dovichi, N. J. *J. Chromatogr.* **1989**, *480*, 141−155.
(30) Matthews, T. G.; Lytle, F. E. *Anal. Chem.* **1979**, *51*, 583−585.
(31) St. John, P. A.; McCarthy, W. J.; Winefordner, J. D. *Anal. Chem.* **1966**, *38*, 1828−1835.
(32) Walrafen, G. E. *J. Chem. Phys.* **1964**, *40*, 3249−3256.
(33) Walrafen, G. E.; Stone, J. *Appl. Spectrosc.* **1975**, *29*, 337−344.
(34) Amirkhanian, V.; Deliwala, S. S.; Franck, R. W.; Wanders, B. J.; Tepermeister, G. Patent US 6,184,990 B1, 2001.
(35) Mogilevsky, R.; Nedilko, S.; Sharafutdinova, L.; Burlay, S.; Sherbatskii, V.; Boyko, V.; Mittl, S. *Phys. Status Solidi C* **2009**, *6*, S179−S183.
(36) Semrock, Inc. Semrock 2017 Master Catalog. https://www.semrock.com/Data/Sites/1/semrockpdfs/SemrockCatalog.pdf (accessed August 1, 2017).
(37) ICH Harmonised Tripartite Guideline: Validation of Analytical Procedures: Text and Methodology, 1996. http://www.ich.org/fileadmin/Public_Web_Site/ICH_Products/Guidelines/Quality/Q2_R1/Step4/Q2_R1__Guideline.pdf (accessed August 1, 2017).
(38) Hirschfeld, T. *Appl. Opt.* **1976**, *15*, 3135−3139.
(39) Peck, K.; Stryer, L.; Glazer, A. N.; Mathies, R. A. *Proc. Natl. Acad. Sci. U. S. A.* **1989**, *86*, 4087−4091.
(40) Johnson, I. D.; Spence, M. T. Z. *The Molecular Probes Handbook: A Guide to Fluorescent Probes and Labeling Technologies*, 11th ed.; Life Technologies Corporation, 2010. http://www.thermofisher.com/ca/en/home/references/molecular-probes-the-handbook.html (accessed August 1, 2017).
(41) Pauli, J.; Pochstein, M.; Haase, A.; Napp, J.; Luch, A.; Resch-Genger, U. *ChemBioChem* **2017**, *18*, 101−110.

DOI: 10.1021/acs.analchem.7b03400
Anal. Chem. 2017, 89, 11122−11128

Electronic Supporting Information

Improvement of LOD in Fluorescence Detection with Spectrally Non-Uniform Background by Optimization of Emission Filtering

Victor A. Galievsky, Alexander S. Stasheuski, and Sergey N. Krylov*

Department of Chemistry and Centre for Research on Biomolecular Interactions, York University, Toronto, Ontario M3J 1P3, Canada

Corresponding Author
*E-mail: skrylov@yorku.ca.

Abstract. This Supporting Information section contains experimental dependences obtained for commercial CE-instrument with the original emission filter: 1) background on laser power; 2) noise on optical background; 3) signal, noise, and SN_BR on fluorescein concentration. Background spectra are shown both for commercial and custom-made CE instruments. Parameters of optimal spectral filter are calculated for different fluorescein concentrations, and SNR is plotted for 1 pM and 4 nM fluorescein concentrations. SNR and SN_BR dependences on fluorescein concentration are calculated for the optimal 530/40 nm bandpass filter. Typical electropherograms for 1 pM fluorescein concentration obtained with the 530/40 nm bandpass filter are shown. Example of difference in the SNR value between SNR-optimized and SBR-optimized emission filters is presented. Estimation of shot noise coefficient κ is done based on published parameters for the PMT as well as the electronic amplifier. Calculated noise parameters and SNR components are tabulated. Supporting references are also presented.

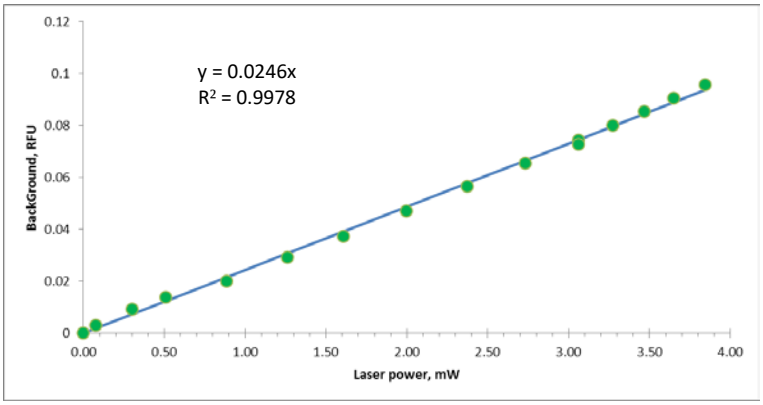

Figure S1. Dependence of optical background signal E_B on 488-nm excitation laser power. Optical power of solid-state continuous-wave laser Whisper IT W488-8PM (PIC, San Jose, CA, USA) was changed by the current-tuning knob of the power supply. The optical background was obtained by subtraction of dark signal value of $E_D = 2.4 \times 10^{-4}$ RFU from the measured LIF signal. Laser power was measured at distal end of optical fiber probe of P/ACE MDQ instrument by Thorlabs power meter PM100A with S130C photodiode sensor.

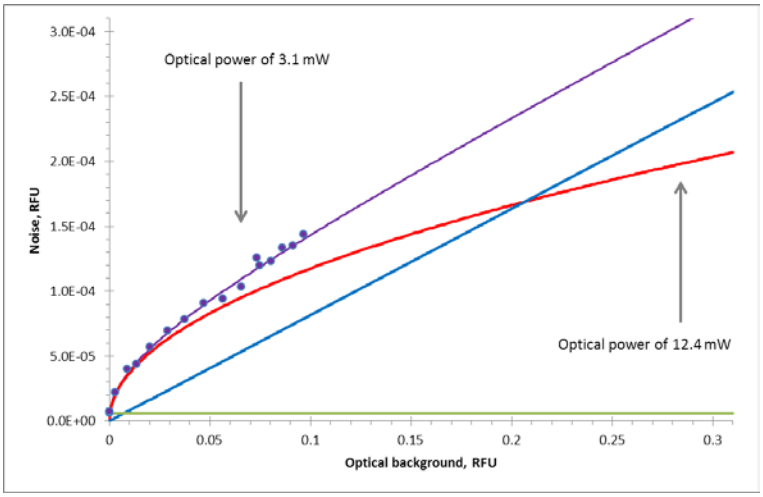

Figure S2. Dependence of noise on the value of optical background E_B (circles). Violet line represents fitting the experimental data by Eq. (7). Red line – the shot noise calculated by Eq. (7) on the assumption that $\chi_B = D = 0$. Blue line – the flicker noise calculated by Eq. (7) on the assumption that $\kappa = D = 0$. Green line – the dark noise calculated by Eq. (7) on the assumption that $\kappa = \chi_B = 0$. An arrow shows the optical background at the default excitation power of 3.1 mW ($E_B = 0.068$, $N = 0.00011$), which is used for everyday measurements at P/ACE MDQ instrument. At this excitation power the relative contributions of shot, flicker and dark noise components to the optical background noise are 16:9:1, respectively. A fourfold increase in the optical power ($E_B = 0.272$) will lead to $N = 0.00030$ and SN_BR improvement about 50%.

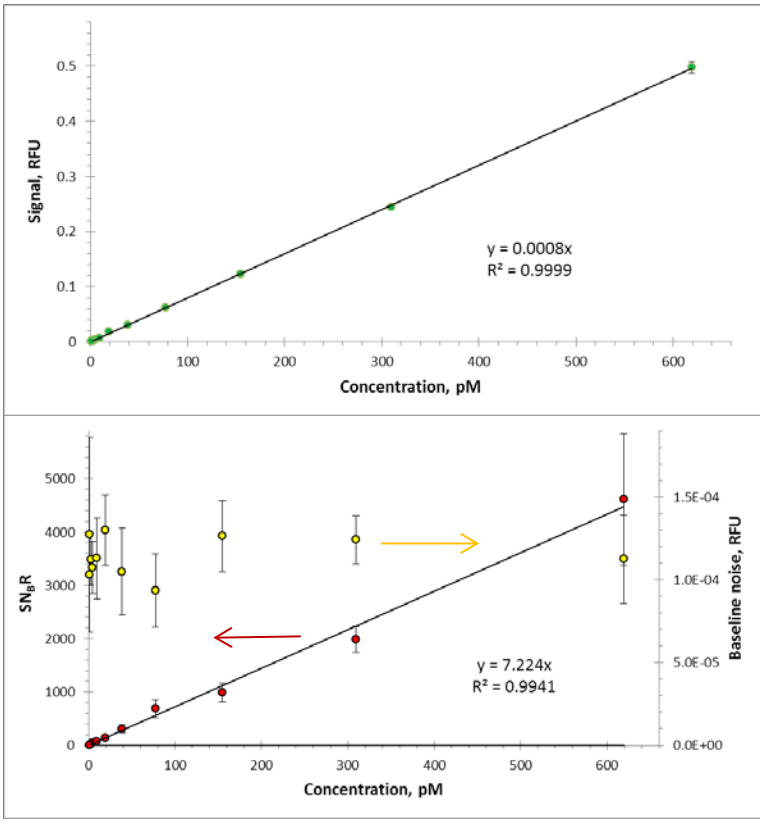

Figure S3. Dependence of CE-LIF signal on fluorescein concentration measured with standard (520/20 nm) fluorescence filter (top). Dependences of signal-to-baseline-noise ratio (SN_BR) and baseline noise on fluorescein concentration (bottom). Laser power was 3.1 mW.

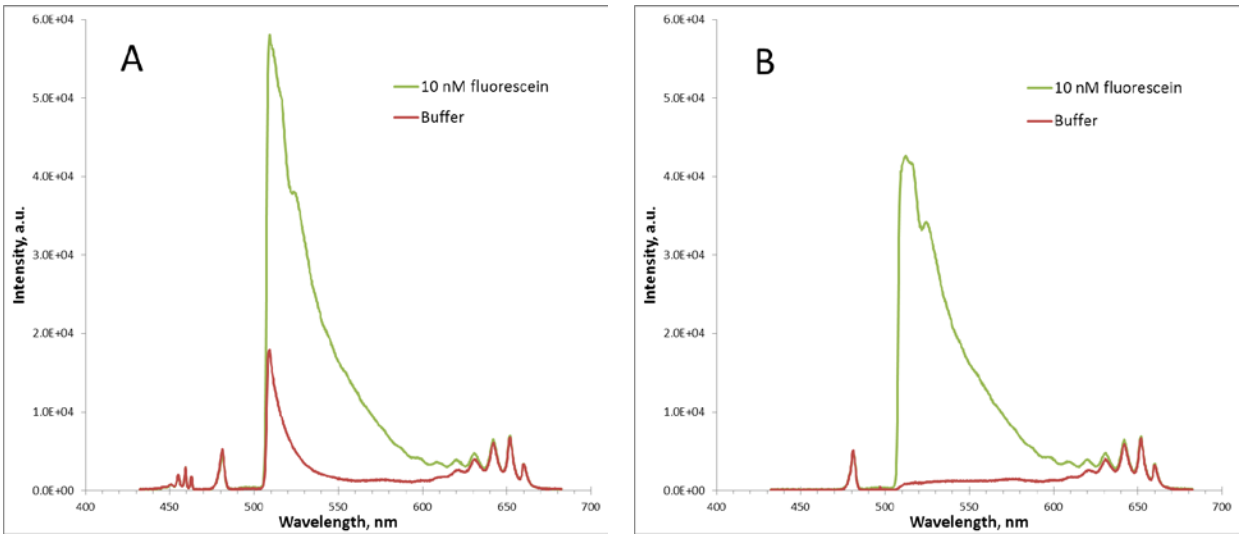

Figure S4. Spectra of 10 nM fluorescein (green line) and Borax buffer (red line) measured without (A) and with (B) an excitation bandpass filter FF02-482/18. A 488-nm solid-state continuous-wave laser Whisper IT W488-8PM was used for excitation; emission was detected by CCD-camera through the 488-nm notch filter.

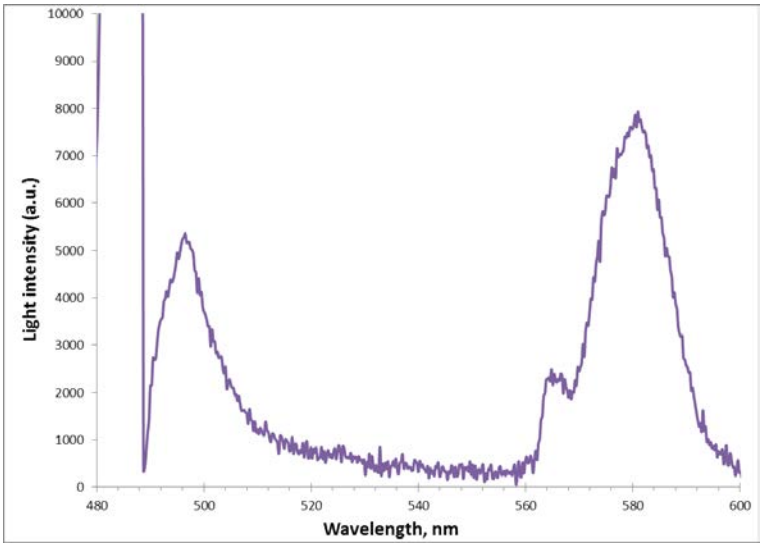

Figure S5. Background spectrum of Borax buffer in the capillary measured in home-made confocal CE-LIF setup. Laser excitation at 485 nm was applied.

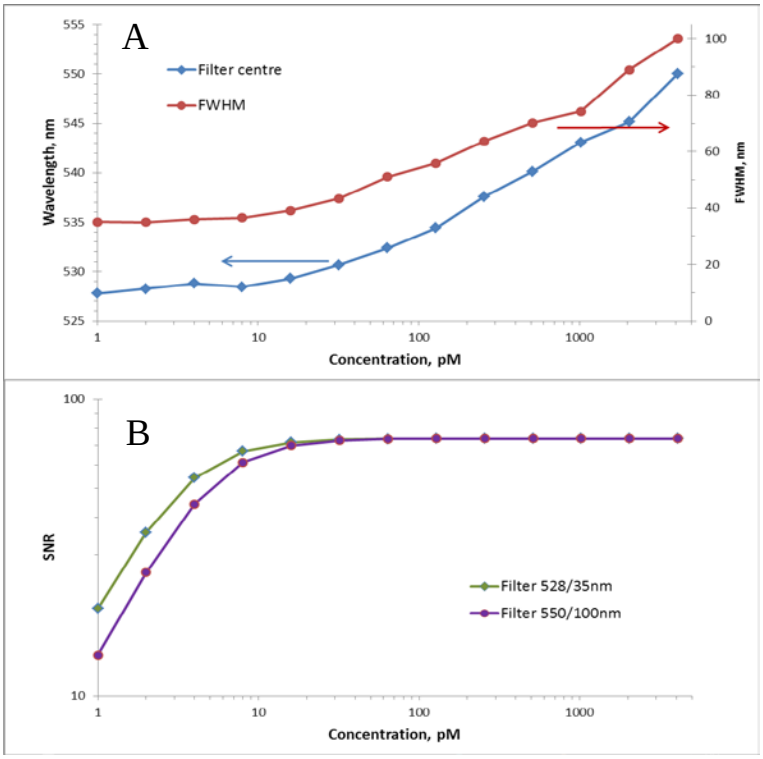

Figure S6. Calculated dependence of optimal filter parameters (filter centre and FWHM) on fluorescein concentration (**A**). Dependences of SNR on fluorescein concentration calculated for filter (optimal for 1 pM concentration) and 550/100 nm (optimal for 4 nM concentration) (**B**). SNR gain of the wider filter (550/100 nm) vs. the narrow filter (528/35 nm) is only 0.001% for the high concentration range.

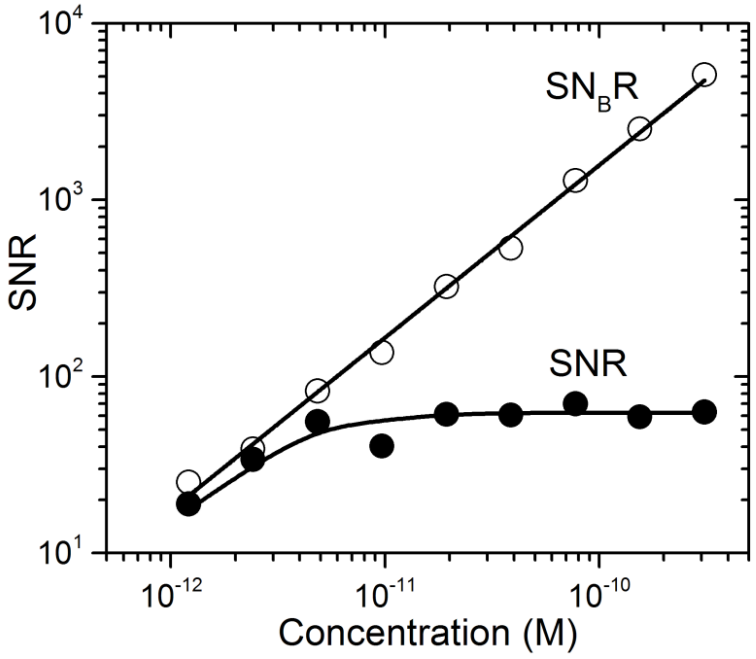

Figure S7. Dependences of SNR and SN_BR on fluorescein concentration measured on CE-LIF instrument using filter 530/40 nm.

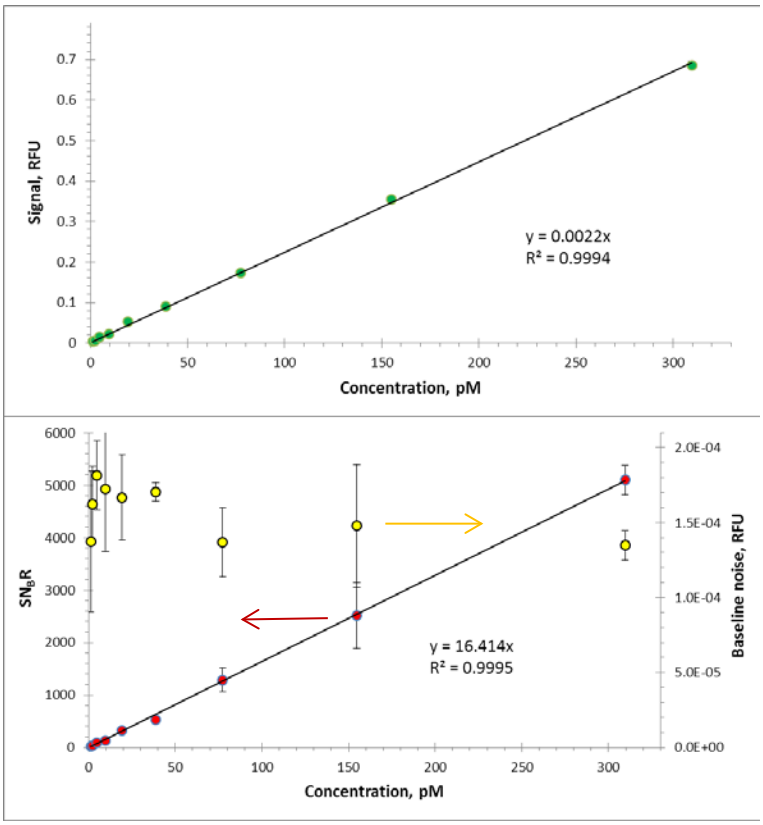

Figure S8. Dependence of CE-LIF signal on fluorescein concentration measured with a 530/40 nm fluorescence filter set (top). Dependences of SN_BR and baseline noise on fluorescein concentration (bottom). Laser power was 3.1 mW.

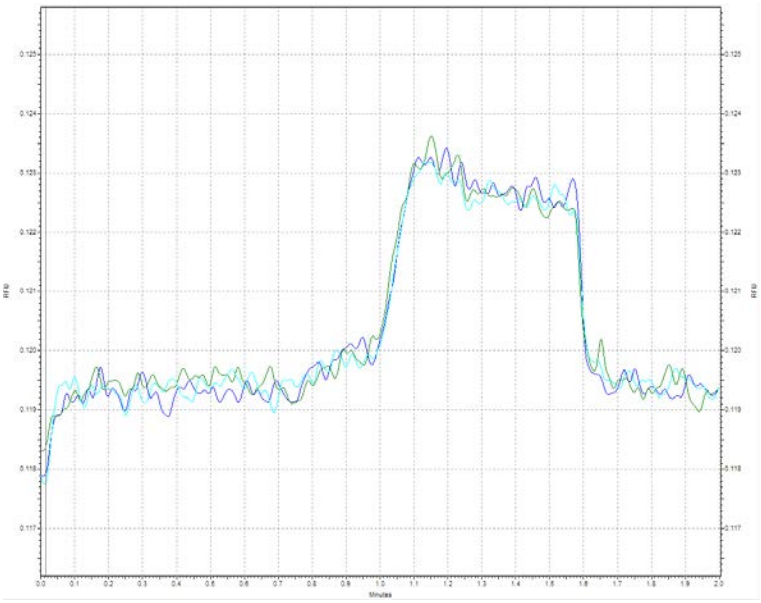

Figure S9. Typical electropherograms of 1 pM fluorescein solution in 25 mM Borax (pH 9.2) measured successively on Beckman CE-LIF instrument using new filter (530/40 nm). The samples were injected into the capillary by a 0.5 psi pressure during 40 s. Electrophoresis was carried out with an electrical potential of +25 kV applied to the injection end of the capillary.

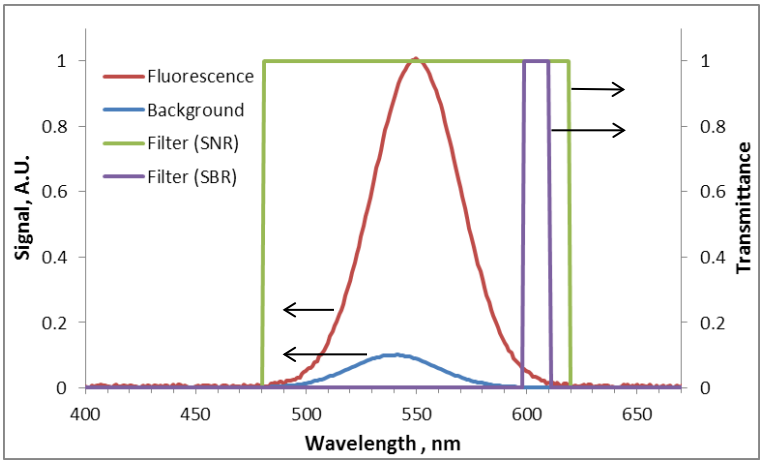

Figure S10. Fluorescence (red curve) and background (blue curve) spectra are modeled by Gaussian functions with means of 550 and 540, respectively. The standard deviation of the Gaussian distribution equals 20. Random noise with maximal amplitude of 1% of Gaussian apex was added to the modeled signals. The maximization of signal-to-noise ratio (SNR), according to the procedure described in the article, gives an optimal filter with a bandpass centre at 550 nm and a width of 140 nm (green curve). For simplicity, it is assumed that there were no dark and flicker noises ($N_D = \chi_S = \chi_B = 0$) and $\kappa = 1$ in Eq. (11). The maximization of signal-to-background ratio (SBR) gives an optimal filter with a bandpass centre at 604 nm and a width of 12 nm (purple curve). SNR calculated by Eq. (11) for the filter 550/140 nm is about 11 times better than that for the filter 604/12 nm, whereas SBR for the filter 550/140 nm is about 3 times worse than that for the filter 604/12 nm.

Table S1. Estimation of shot noise coefficient κ (Eq. (6)) from the PMT and electronic amplifier parameters

Parameter	Value	Comments
α	0.82	PMT coefficient was found in label on a back side of the CE-LIF module of P/ACE MDQ
V, V	703.7	PMT voltage was read from the instrument EEPROM through the COM port (command "eeget" in HyperTerminal)
m	7.49×10^5	PMT gain was calculated by Eq. (S-2) [1]
G, $A^{-1}V$	10^7	Gain of the current-to-voltage converter. It is equal to value of the negative feedback resistor (10^7 Ohm) in the operational amplifier circuit.
η	4.49	PMT gain per dynode stage Eq. (S-3) [2]
δ	0.29	$\delta^{0.5}$ is a fraction of the quantum noise in the anodic current Eq. (S-4) [2]
e, C	1.6×10^{-19}	Electron charge
τ, s	0.5	Time-constant of low-pass electronic filter in CE-LIF detection. This parameter was estimated indirectly from the instrument acquisition frequency of 4 Hz. According to the Nyquist–Shannon–Kotelnikov sampling theorem [3] the acquisition frequency should be at least twice the cut-off frequency of low-pass filter.
Δf, Hz	0.5	Noise equivalent bandpass Eq. (S-5) [2]
K, A	2.06×10^{-19}	Bandwidth constant Eq. (S-6) [2]
κ, V	1.5×10^{-6}	Eq. (S-7) [2]
ADC range, V	10	We supposed voltage range of 0−10 V for ADC CS5016-JL32 used in the CE-LIF module of P/ACE MDQ
Dynamic range of detector, RFU	1	Acquisition dynamic range in the detector settings (32 Karat v.7.0 acquisition software) was set to 1 RFU. Dynamic range in RFU corresponds to ADC range in V.
κ, RFU	1.5×10^{-7}	Shot noise coefficient κ in Eq. (6)

$$m = A^n \left[\frac{V}{(n+1)} \right]^{\alpha n} \tag{S-1}$$

Gain *m* of PMT can be calculated by Eq. (S-1) (ref. [1]), where *A* is a constant, *V* is a voltage applied between the cathode and the anode of the PMT having *n* dynode stages, α is a coefficient determined by the dynode material and geometric structure. According to specification the PMT Hamamatsu R5984 contains 9 dynode stages and has gain 10^7 at applied voltage 1000 V that corresponds to coefficient *A* of 1.74×10^{-8}. So PMT gain *m* is equal to:

$$m = 1.74 \times 10^{-8} \left(\frac{V}{10} \right)^{9\alpha} \tag{S-2}$$

$$\eta = 10^{\left(\frac{\lg m}{9} \right)} \tag{S-3}$$

$$\delta = \frac{1}{\eta - 1} \tag{S-4}$$

$$\Delta f = \frac{1}{4\tau} \tag{S-5}$$

$$K = 2e\,\Delta f\,(1+\delta) \tag{S-6}$$

$$\kappa = mGK \tag{S-7}$$

Table S2. Noise parameters and SNR components

Term	Value	Description
κ	$1.4(4) \times 10^{-7}$ RFU	Coefficient determining shot noise
χ_B	$8(3) \times 10^{-4}$	Flicker factor for background signal
χ_S	$1.4(4) \times 10^{-2}$	Flicker factor for analyte signal
N_D	$6.1(3) \times 10^{-6}$ RFU	Dark noise, $(\kappa E_D + \sigma_{dex}^2 + \sigma_{ar}^2)^{0.5}$
N_B[a]	$1.1(2) \times 10^{-4}$ RFU	Optical background noise, $(\kappa E_B + (\chi_B E_B)^2)^{0.5}$
N_S[a]	$2.1(5) \times 10^{-5}$ RFU	Optical analyte noise, $(\kappa E_S + (\chi_S E_S)^2)^{0.5}$
N	$1.1(2) \times 10^{-4}$ RFU	Total noise, $(N_D^2 + N_B^2 + N_S^2)^{0.5}$
SNR	11(2)	E_S/N
SN_BR	11(2)	$E_S/(D^2 + N_B^2)^{0.5}$

[a]Noise components N_B and N_S are presented to demonstrate their relative contributions into the total noise N. Noise was calculated for the following signals: E_B = 0.068(6) RFU (laser power of 3.1 mW) and E_S = 0.0012(2) RFU (fluorescein of 1 pM).

References

(1) Hamamatsu Photonics, Photomultiplier Tubes. Basics and applications (Available from: http://www.hamamatsu.com/resources/pdf/etd/PMT_handbook_v3aE.pdf), Hamamatsu Photonics K.K., 2007.
(2) Ingle, J. D.; Crouch, S. R. Signal-to-Noise Consideration. In *Spectrochemical Analysis*; Prentice-Hall, Inc.: New Jersey, 1988, pp 135-163.
(3) H.D. Luke, The origins of the sampling theorem, IEEE Commun Mag, 37 (1999) 106-108.